Crystallization Kinetics and Degradation of Nanocomposites Based on Ternary Blend of Poly(L-lactic acid), Poly(methyl methacrylate), and Poly(ethylene oxide) with Two Different Organoclays

Andi Auliawan, Eamor M. Woo

Department of Chemical Engineering, National Cheng Kung University, Tainan 701, Taiwan

Received 13 September 2011; accepted 5 January 2012
DOI 10.1002/app.36761
Published online in Wiley Online Library (wileyonlinelibrary.com).

ABSTRACT: Ternary polymer blends composed of poly(L-lactic acid) (PLLA), poly(methyl methacrylate) (PMMA), and poly(ethylene oxide) (PEO) is used as matrix for nanocomposites with two clays: organically modified vermiculite (OVMT) and organically modified montmorillonite (Clo10A). The addition of PMMA in PLLA/PEO blend matrix reduces the chain mobility and retards the crystallization of PLLA/PEO. The retardation effect of PMMA on PLLA/PEO blend is less pronounced with higher PEO contents. The incorporation of OVMT and Clo10A is one common strategy to improve crystallization process as well as thermal and mechanical properties. The crystallization kinetics of polymer nanocomposites was found to be well described by the Mo method. The evolution of activation energy during nonisothermal course is analyzed using isoconversional method, and the trend of activation energy variation was found to be different for each of two organoclays. Thermal stability is improved by the incorporation of organoclays, where Clo10A induces better stability than that of OVMT. Enzymatic degradation tests showed that the nanocomposites with OVMT possessed higher stability on enzymatic attack and slower degradation. © 2012 Wiley Periodicals, Inc. J Appl Polym Sci 000: 000–000, 2012

Key words: ternary polymer blend; organoclays; nonisothermal crystallization; activation energy; enzymatic degradation; thermal stability

INTRODUCTION

During the last decade, biodegradable polymers have attracted more interest due to increasing environmental awareness and decreasing nonrenewable resources. For these reasons, many researches have been conducted by academic and industrial party to develop environmental-friendly materials. Biopolymers are materials which can be derived from renewable resources such as agricultural resources. Biopolymers represent alternative choice to replace common nonbiodegradable polymers for short-life range application. In practical, most biodegradable polymers are costly compared with conventional thermoplastic, and their properties are sometimes not sufficient for practical applications.[1]

Poly(lactic acid) (PLA) is one example of biodegradable polyesters which can be obtained from agricultural stocks, such as corn, potato, and sugar cane. PLA exists in L-form and D-form optical isomers. PLA with mainly L-form isomer (PLLA) is highly crystalline. L/D-PLA is used widely in biomedical applications for drug delivery, medical implants, and surgical sutures.[2,3] PLA has several advantages, which are environmental-friendly, better processability in comparison with other biopolymers, and more energy saving in production than petroleum-based polymers.[4–6] PLA also exhibits biocompatibility and high mechanical performances comparable with those of some petroleum-based polymers.[7] PLA is a transparent and crystalline polymer with relatively high melting point but brittle properties. It has high strength and low elongation at break.[8] The main disadvantages of this biodegradable polymer are its poor thermal stability, mechanical resistance, and limited gas barrier properties, which limit its use in the industrial applications.[9] PLA also has slow degradation rate; PLA degrades through the hydrolysis of backbone ester groups and the degradation rate is dependent on PLA's degree of crystallinity, molecular weight, morphology, water diffusion rate into the polymer, and the stereoisomeric content.[10]

Several ways can be attempted to enhance the properties of polymers. Blending, copolymerization, and introducing filler to polymer matrix are the common used method. Poly(ethylene oxide) (PEO) is

Correspondence to: E. M. Woo (emwoo@mail.ncku.edu.tw).

Contract grant sponsor: Taiwan's National Science Council (NSC); contract grant number: NSC-97-2221-E-006-034-MY3

a crystalline polymer, highly biocompatible and pharmacologically inactive water-soluble polymer.[11] The incorporation of PEO is reported to increase the biodegradability in PLLA/PEO blends.[12] It has also been reported that the addition of poly(methyl methacrylate) (PMMA) can enhance the exfoliation of silicate layers.[13] Thus, blending of PEO, PMMA with PLLA and clays is expected to more versatile in improving and broadening the PLLA applications as matrix materials for nanocomposites with balanced matrix properties and better clay intercalation.

The addition of filler, i.e., clay minerals in a small amount can enhance thermal and mechanical properties of the polymer. The most common clays used are based on montmorillonite (MMT), hectorite, and saponite. Polymer/clay nanocomposites can be prepared via *in situ* intercalative polymerization of monomers, polymer intercalation by solution intercalation and melt intercalation methods.[14] Vermiculite (VMT) is another type of clay which is abundant, cheaper and has larger cation exchange capacity than the commonly used MMTs. Both VMT and MMT belong to the family of 2 : 1 layered silicates. VMT is generally used in packaging for antishocking purposes. This clay contains either Al^{3+} or Mg^{2+} and Fe^{2+} as normal octahedral ions, and a tetrahedral sheet in which Al^{3+} occurs as a substituted ions in place of some of the Si^{4+} ions.[15]

Ternary polymer blends as matrix materials for nanocomposites were a novel attempt custom-tailoring biocompatibility, physical properties, dispersion of clays in matrix, optimal kinetics for processing, etc. In this study, PLLA was modified by blending with two polymers: PMMA and PEO, and reinforced with organically modified clays (OVMT and OMMT). The thermal behavior of ternary polymer blends and crystallization kinetic of the organoclay-modified ternary polymer blend are discussed. Effects were discussed on organically modified clays introduced to the polymer mixtures to produce a ternary polymer/clay nanocomposite. Different effect of organoclay loading on the interaction with polymer matrix as well as kinetics and properties of the unique ternary polymer/clay nanocomposites were investigated. As the degradation ability is one of the important issue in developing environmentally friendly materials, the enzymatic degradation test was performed to investigate the effect of different organoclays on degradation process of polymer nanocomposites. Thermal degradation test was also performed to observe the extent of stability induced by organoclays.

EXPERIMENTAL

Materials

Poly(L-lactic acid) (PLLA) from NatureWorks® (Blair, Nebraska, USA) (M_w 119,400; T_g 58.8°C and T_m 165.3°C), PMMA from Chimei (Tainan, Taiwan) with code name CM-205 (M_w 53,500; T_g 105°C), and PEO from Aldrich (Buchs, Switzerland) (M_w 200,000; T_g −58.8°C and T_m 64°C) were used as polymer matrix materials. VMT grade No. 3 from Sigma-Aldrich (Buchs, Switzerland) (VMT equivalent weight of 50–150 mmole/100 g, M_w 504.19) was used as the filler to form polymer nanocomposites as well as Cloisite10A®. Hexadecyltrimethylammonium bromide (HDTMAB) from Alfa Aesar (Heysham, Lancashire) (FW 364.46) was used as an organic modifier for VMT. Another type of clay, Cloisite10A®, was purchased from Southern Clay Product (Widnes, Cheshire, UK), with dimethyl benzyl hydrogenated tallow quaternary ammonium ion (2MBHT) as the modifier. The modifier concentration on Cloisite10A® is about 125 meq/100 g clay, and the hydrogenated tallow consisting of ca. 65% C18, ca. 30% C16, and ca. 5% C14. Cloisite10A® has interlayer spacing (d_{001}) of 19.2 Å. Cloisite10A® term is abbreviated as Clo10A throughout this study. Proteinase-K enzymes from *Tritirachium Album* and Tris buffer for enzymatic degradation test were purchased from Sigma-Aldrich.

VMT modification

Modification of VMT can be performed using maleic anhydride, acid, sodium, and long chain quaternary ammonium salts.[16–19] In this study, VMT clay was organically modified using HDTMAB, which is a quaternary ammonium salt. This modifier allows alkyl ammonium chain to be inserted into VMT gallery. Procedures are as following. 8.5 g grounded VMT was mixed with 300 mL, 4 wt % HDTMAB. The suspension was then stirred at 80°C for 1 day to promote ionic exchange reaction. To recover the solid, the suspension was then filtered using filter paper and washed with double distilled water. The filtrate was washed and then titrated with 1 wt % $AgNO_3$ solution. The washing procedure was repeated until no white precipitate left on titration with $AgNO_3$ solution. The solid filtrate was then dried in oven at 100°C for 48 h before use, and the dried solid was kept in the oven for future use. The organically modified VMT was then abbreviated as OVMT throughout this study.

Sample preparation

To study the effect of organoclay loading on the crystallization of polymer blend, the thoroughly dried organoclays and polymers were dry-mixed at four different clay loadings of 1, 3, 5, and 8 wt %. The polymer blend compositions were at 80, 10, and 10 wt % of PLLA, PMMA, and PEO, respectively. The mixtures were then prepared by melt intercalation method at 190°C under nitrogen flow to avoid thermal degradation. Melt-blending was performed by placing a small quantity of sample (1 g total of

mixtures) in a temperature-controlled (~ 160–170°C) and dry-nitrogen-purged mold, where shear forces for thorough mixing were imposed by vigorous and continuous hand stirring. The mixtures of small quantities at $T = 160$–170°C had low viscosity, which could be conveniently handled by manual stirring. The polymer nanocomposites were then cooled down to room temperature. All samples for crystallization studies were cut as thin films from the bulk nanocomposite samples. For enzymatic and thermal degradation tests, the polymer nanocomposites at different organoclays loading of 1, 3, 5, and 8 wt % were pressed as thick film squares with 10 mm × 10 mm × 0.3 mm in dimensions.

Characterization

Differential scanning calorimetry

Perkin-Elmer (Massachusetts, USA) differential scanning calorimetry (DSC)-Diamond was used for nonisothermal crystallization experiments. All samples were heated to 200°C and maintained at that temperature for 3 min to completely melt the polymer crystals. Then, the samples were cooled to −62°C at the rates of 2.5°C/min, 5°C/min, 10°C/min, 15°C/min, and 20°C/min, respectively. The subsequent melting behavior of each sample was recorded at the heating rate of 2.5°C, 5°C, 10°C, 15°C, and 20°C, respectively.

Transmission electron microscopy

A JEOL JEM 1200-EX (Tokyo, Japan) transmission electron microscopy (TEM) instrument was used. All samples were epoxy coated and ultra-microtomed with a diamond knife on a Leica Ultracut R microtome to make sections with a nominal thickness of 40 nm. These sections were then transferred to carbon-coated 200 mesh Cu grids. TEM images were obtained at accelerating voltage of 80 kV.

Scanning electron microscopy

FEI Quanta-400F (Hillsboro, Oregon, USA) scanning electron microscopy (SEM) was used to observe the surface morphology of polymer nanocomposites before and after specific enzymatic degradation course. All samples were gold coated before SEM observation.

Thermogravimetric analysis

Thermogravimetric analysis (TGA) TA Q-50 (New Castle, Delaware) was used for observation of thermal stability in polymer nanocomposites. TGA scans were recorded at a heating rate of 10°C/min under a flow of N_2 in the temperature range of 40°C to 800°C. All samples were dried before TGA measurement.

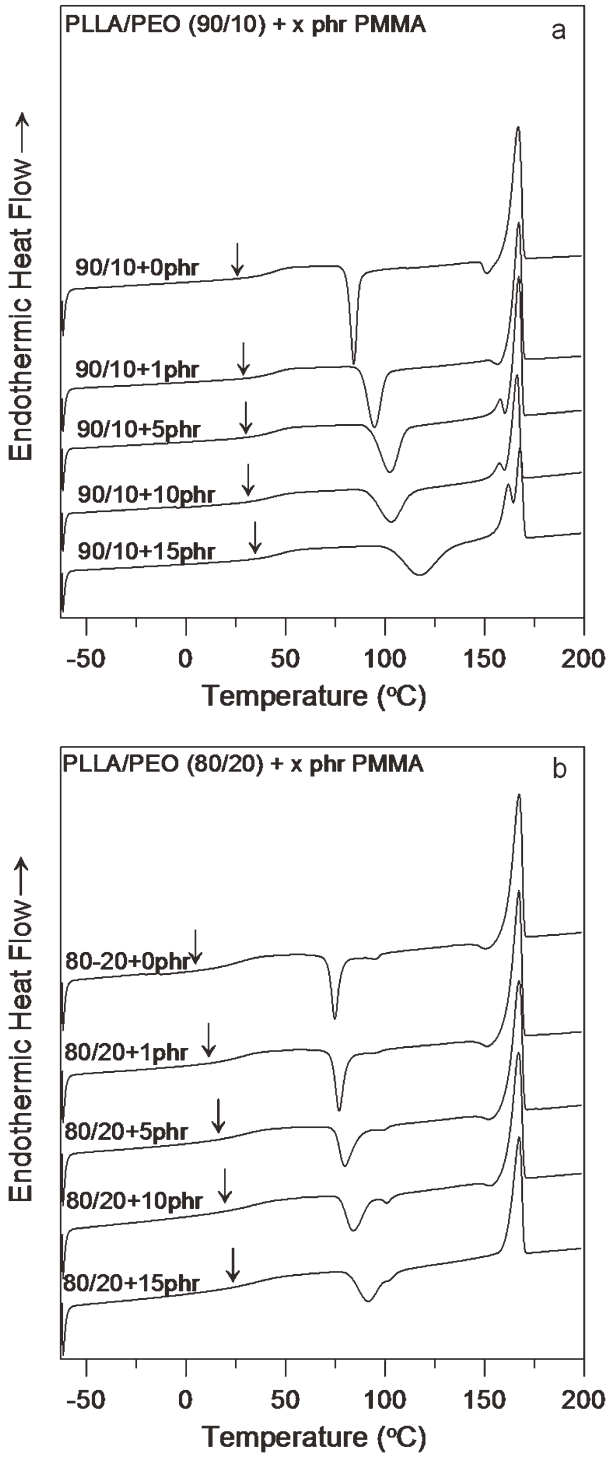

Figure 1 DSC curves for ternary blend comprising fixed content of PLLA/PEO blend matrix: (a) 90/10 and (b) 80/20 with various PMMA contents (parts per hundred parts of PLLA/PEO).

RESULTS AND DISCUSSION

Effect of PMMA addition on thermal behavior of PLLA/PEO

Figure 1(a) presents DSC scan for melt quenched samples comprising fixed compositions of PLLA/

PEO (90/10) and (80/20) with incorporation of increasing PMMA content. The figure shows that T_g of the blend is slightly increased with the addition of PMMA. The T_{cc} of the blend is also shifted to higher temperature along with increasing PMMA, the T_{cc} peak also broadens and has a lower peak height (lower exothermic peak). In 90/10 blend, the addition of 1 phr PMMA significantly shifts T_{cc} to a higher temperature, indicating that the addition of PMMA can induce significant retardation effect on the blend. At PMMA compositions of 0 and 1 phr in ternary blend, small exothermic peaks are observed in DSC traces. These peaks may arise from the recrystallization of PLLA after melt-quenching process. The crystals formed during melt-quenched process is less perfect, thus the crystals then melt and recrystallize again on heating to form more perfect crystals. However, only a small portion of PLLA chains can crystallize from melt-quench condition. The existence of recrystallization peaks show that on addition of 1 phr PMMA into PLLA/PEO (90/10) blend, the polymer chain still have the mobility which enable them to form crystals during melt-quenched process. In other words, the retardation effect of PMMA is not strong enough to completely block the PLLA chain mobility in the PLLA/PEO (90/10) blend. Further addition of PMMA into PLLA/PEO (90/10) blend results in appearance of small endothermic peak at around 160°C, thus from the DSC scans, double melting peaks appear. The intensity of this small peak also increases with higher content of PMMA in blends. As the double melting peak corresponds to melt and recrystallization phenomenon,[20] the occurrence of small endothermic peak can be attributed to formation of less perfect crystals on heating. And as the intensity of this peak increases with higher content of PMMA, it can be concluded that the addition of PMMA will lead to formation of less perfect crystals on heating. From Figure 1(b), all the samples reveals recrystallization peak, except for the sample containing 15 phr PMMA. The existence of recrystallization peaks may be attributed to better chain mobility of PLLA in comparison with that of PLLA/PEO (90/10). From the result, it can be concluded that in the PLLA/PEO (80/20) blend, the retardation effect of PMMA is not strong enough, as more content enhances the plasticization effect on PLLA. Therefore, in this blend, PLLA chains have better chain mobility. However, the T_{cc} peaks broaden and have lower intensity as the PMMA content increases, showing that PMMA still has effect or interaction on the PLLA/PEO (80/20) blend. The values of T_g and T_{cc} slightly increase with increasing PMMA content, indicating intimate interactions in the blend of a miscible state.

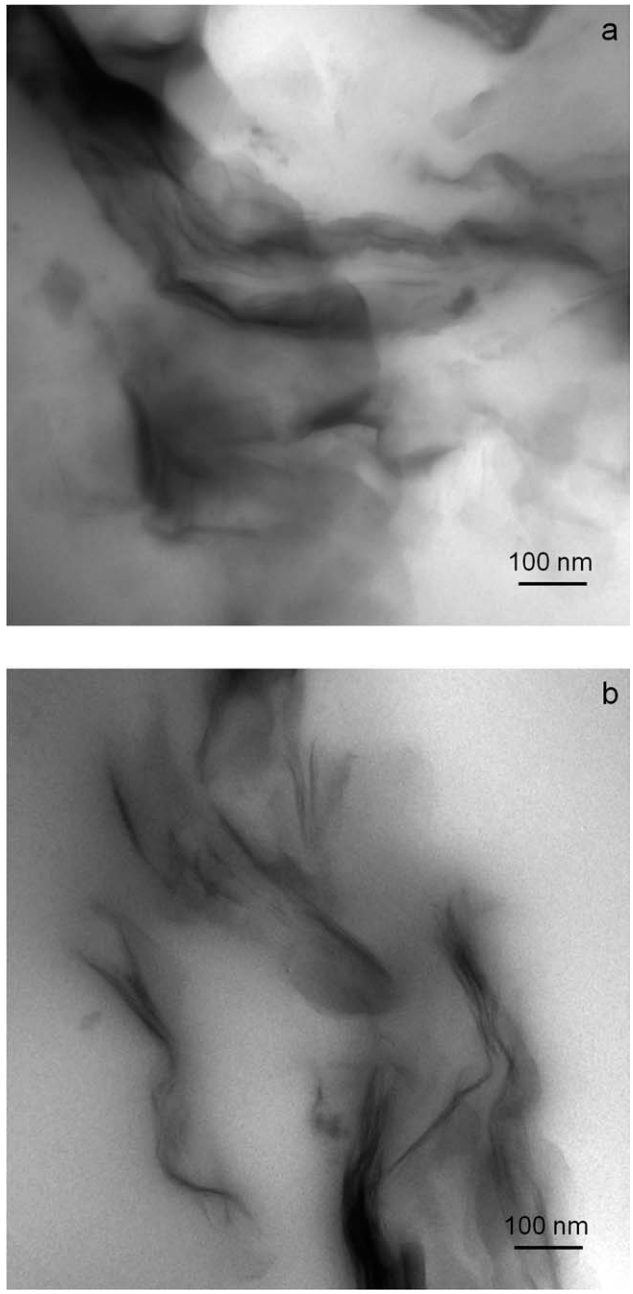

Figure 2 TEM images of PLLA/PMMA/PEO (80/10/10) blend nanocomposites with (a) 3% OVMT and (b) 3% Clo10A.

Organoclays dispersion in polymers matrix

TEM observation was used to observe the dispersion of organoclays in polymer blend matrix. Figure 2 shows TEM images for the polymer nanocomposites of PLLA/PMMA/PEO with two different organoclays. OVMT has more disordered organoclays structures, which indicates that the pristine organoclay structure already disrupted. Some intercalated parts and organoclays aggregates are also found in OVMT nanocomposites as in Figure 2(a). In Clo10A, the organoclays structures are more ordered than

that of OVMT. However, some disordered parts and aggregates also can be found in Figure 2(b). The intercalation of Clo10A is more pronounced than that of OVMT as shown in Figure 2(b). Regarding the wide angle x-ray diffraction (WAXD) and TEM observation for the dispersion of two different organoclays in PLLA/PMMA/PEO nanocomposites, the dispersed organoclays particles can be considered to have a good dispersion in the polymers matrix, both of OVMT and Clo10A. The TEM result of CLo10A clay dispersion in the ternary blend matrix is quite similar to OVMT clay in the matrix, as demonstrated in concurrent work published earlier.[21]

Nonisothermal crystallization behavior

Nearly in every melt processing, the molten polymer is subjected to shearing and nonisothermal conditions. Thus, the study related to the kinetics of crystallization is an important key to correlate between processing and properties of polymers. Regarding to those facts, an understanding of nonisothermal crystallization behavior is of practical importance. In this study, nonisothermal crystallization was also performed to investigate the effect of clay loading during nonisothermal crystallization process. The nonisothermal crystallization behavior for neat PLLA/PMMA/PEO (80/10/10) and its nanocomposites of 3% Clo10A are shown in Figure 3. For the neat ternary polymer blend (without organoclays), the nonisothermal crystallization peak is hardly observed even with cooling rate as low as 2.5°C/min. This result suggests that the crystallization process of neat ternary blend during nonisothermal process is very difficult. This fact may be due to the lack of time needed for crystallization process. During the nonisothermal course, the time for crystallization process is limited by the T_g of the polymer blend. As the temperature during cooling is always continuously lowered with time, when the T_g is reached, the molecular movement/mobility is frozen. Thus, no molecular arrangement or crystallization was possible as temperature was lowered to below T_g. On addition of organoclays, the clear crystallization peak can be observed during cooling. The crystallization peak is shifted to lower temperature as higher cooling rate applied, as shown in Figure 3(b). In addition to that, the molecular chain become less flexible, less mobile and has shorter time to diffuse into the crystalline lattice. The molecular chain also has shorter time to adjust and organize the chain configurations into more perfect crystallites. As a result, the extent of crystallite perfection also decreased with faster cooling rates.[22] The shift of crystallization peak indicates that the higher the cooling rate, the crystallization process starts and is completed in later period.[23] The shift of crystallization peak to lower temperature is also followed by the shifts of some parameters such as crystallization onset and half time crystallization. Figure 4 presents the heat evolution of nonisothermal crystallization of neat ternary blend and its nanocomposites at the rate of 5°C/min. During cooling, no exothermic peak is observed for neat polymer blend. The crystallization process of neat polymer blend is either difficult or may be took place in a very broad temperature range. On heating for neat ternary blend, cold crystallization peak is clearly observed at around 84°C, which indicates the molecular

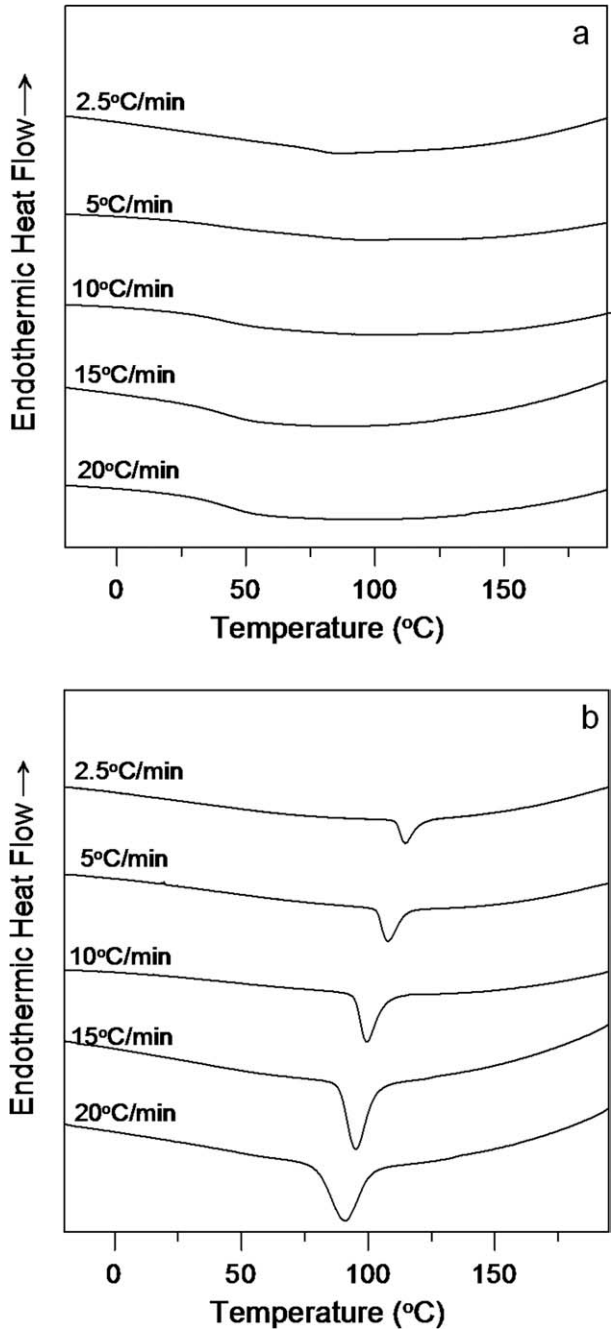

Figure 3 DSC cooling scan of PLLA/PMMA/PEO (80/10/10): (a) without organoclay and (b) 3% Clo10A.

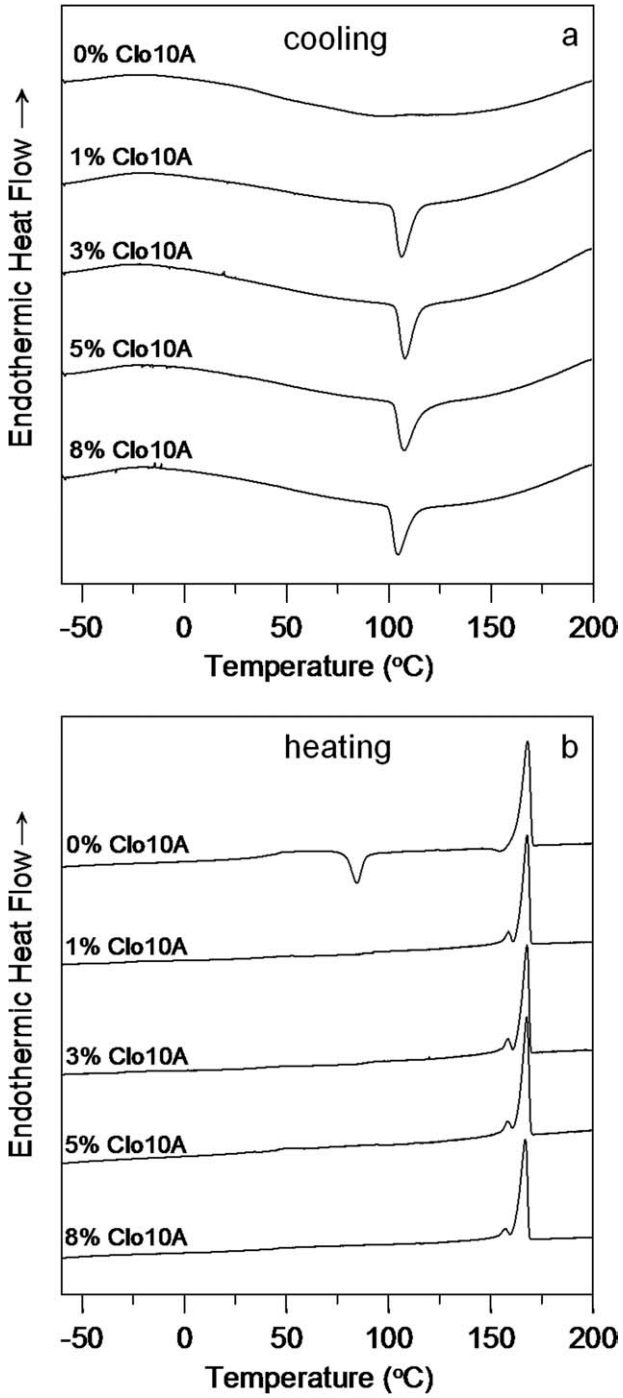

Figure 4 (a) Initial DSC cooling scans and (b) subsequent heating scans of PLLA/PMMA/PEO (80/10/10)+3% Clo10A at rate of 5°C/min.

arrangement of polymer chains during crystallization. The recrystallization peak at around 154°C is also observed, which indicates some degree of crystallization during cooling. On addition of 1% organoclay loading, dramatic change in DSC cooling curve takes place. The sharp exothermic peak of crystallization can be clearly observed. For all nanocomposites DSC curves, on heating, there is no cold crystallization peak observed, which indicates that the crystallization process already completed during cooling. All the heating scan curves show double melting peak, indicating a process of melting–recrystallization–remelting phenomena of PLLA.[20]

The trend of increasing organoclay loading is different between OVMT and Clo10A. Further addition of OVMT higher than 1 wt % leads to direct decrease of T_p (crystallization peak temperature). While for Clo10A, the increase Clo10A loading from 1 wt % will lead to the increase of T_p before bouncing to lower temperature at around Clo10A loading 3–5 wt %. During nonisothermal crystallization course, the exothermic peak which exists at higher temperature indicates the crystallization process occur easier than that of lower temperature. This is because the molten polymer is directly cooled from the melt condition using certain cooling rate, thus the exothermic peak at higher temperature marks the faster crystallization process. Therefore, apparently further addition of OVMT from 1 wt % directly retards the crystallization process, thus lowered the crystallization peak temperature. In the case of Clo10A, further addition of Clo10A from 1 wt % loading increases the crystallization extent before retards it at 3–5% Clo10A loading. Perhaps, the higher content of Clo10A restricts the molecular chain movement, thus affects the crystallization extent. From the trend of OVMT and Clo10A loading on nonisothermal crystallization, it seems that these organoclays affect the kinetics in different way. Table I for OVMT and Table II for Clo10A summarize the values of T_p and ΔH_m (melting enthalpy) of nanocomposites. The crystallite perfection or the extent of crystallinity, which is represented by ΔH_m, is evidently decreased with increasing cooling rate, as shown in Tables I and II. The melting enthalpy trend is lower (less negative value) as cooling rate increases. The lower cooling rate provides more fluidity and diffusivity for the molecules due to relative lower viscosity and more time to crystallize, thus inducing higher exotherm enthalpy and more perfect crystallization.[24]

Nonisothermal crystallization kinetics

From the data for crystallization exotherms as a function of temperature dH_c/dT, the relative crystallinity as function of temperature, $X(T)$, can be calculated as follows:

$$X(T) = \frac{\int_{T_o}^{T_c} \frac{dH_c}{dT} dT}{\int_{T_o}^{T_\infty} \frac{dH_c}{dT} dT} \quad (1)$$

where, T_o, T_c, and T_∞ denote initial crystallization temperature, crystallization temperature at time t

TABLE I
Parameters of PLLA/PMMA/PEO (80/10/10)+OVMT Nanocomposites Using Nonisothermal Crystallization Analysis

Clay loading	Cooling rate (°C/min)	T_p (°C)	ΔH_c (J/g)	n	Z_t (min^{-n}) × 10^3	Z_c	$t_{1/2}$ (min)
1% OVMT	2.5	121.6	−42.3	4.62	1.372	0.072	5.07
	5	114.8	−41.1	4.10	9.024	0.390	2.91
	10	102.0	−32.1	5.23	14.73	0.656	2.12
	15	98.1	−27.5	4.89	95.61	0.855	1.53
	20	91.8	−23.6	5.28	185.61	0.919	1.29
3% OVMT	2.5	121.4	−41.4	3.93	1.299	0.070	5.15
	5	113.4	−39.5	3.92	8.968	0.390	3.10
	10	99.7	−30.3	5.48	5.68	0.596	2.98
	15	96.5	−27.1	5.67	73.62	0.840	1.58
	20	91.8	−23.6	5.44	114.60	0.897	1.39
5% OVMT	2.5	115.9	−36.2	4.00	0.359	0.042	6.10
	5	109.1	−33.0	4.29	6.286	0.363	3.24
	10	97.0	−26.8	6.20	1.55	0.524	3.12
	15	93.8	−25.0	5.67	47.86	0.817	1.61
	20	90.2	−21.4	5.36	79.67	0.881	1.50
8% OVMT	2.5	119.7	−36.3	3.50	0.498	0.048	5.82
	5	110.2	−34.4	3.62	7.388	0.375	3.18
	10	97.3	−27.5	5.67	3.20	0.563	2.62
	15	94.8	−25.8	5.63	46.49	0.815	1.63
	20	91.2	−22.3	5.41	96.29	0.890	1.44

and crystallization temperature after the completion of crystallization process. Once the $X(T)$ is obtained, the conversion into $X(t)$ can be performed by transforming the temperature axis to time axis using the transformation of $t = (T_o - T)/\alpha$, where α is cooling rate. The Avrami equation can be applied to describe the nonisothermal crystallization behavior. Under nonisothermal crystallization, the Avrami equation could still partly explain the primary stage of crystallization.[25] The Avrami equation is not applicable in the late stages, where secondary nucleation takes place.[26–28] The Avrami equation for nonisothermal crystallization is described as follows:

$$1 - X_c(T) = \exp(-Z_t t^n) \quad (2)$$

$$\log[-\ln\{1 - X_c(T)\}] = n \log t + \log Z_t \quad (3)$$

where n is a parameter depending on the nature of nucleation and growth geometry and is termed as the Avrami exponent, and Z_t is a growth rate constant involving nucleation and growth rate parameters. Jeziorny suggested that the values of Z_t

TABLE II
Parameters of PLLA/PMMA/PEO (80/10/10)+Clo10A Nanocomposites Using Nonisothermal Crystallization Analysis

Clay loading	Cooling rate (°C/min)	T_p (°C)	ΔH_c (J/g)	n	Z_t (min^{-n}) × 10^3	Z_c	$t_{1/2}$ (min)
1% Clo10A	2.5	113.1	−34.2	6.68	0.002	0.006	6.58
	5	106.3	−27.7	5.26	0.937	0.248	3.56
	10	98.2	−21.9	5.30	15.33	0.658	2.08
	15	92.8	−21.0	3.59	529.42	0.958	1.09
	20	88.9	−17.9	3.84	506.64	0.967	1.08
3% Clo10A	2.5	114.7	−39.0	5.50	0.049	0.019	5.74
	5	107.9	−28.8	4.99	1.974	0.288	3.27
	10	99.5	−22.7	5.65	16.49	0.663	1.96
	15	95.3	−21.8	3.83	782.53	0.984	0.97
	20	90.8	−20.7	3.92	730.47	0.984	0.98
5% Clo10A	2.5	114.4	−38.4	4.13	0.832	0.059	5.18
	5	107.3	−27.1	4.35	4.711	0.342	3.24
	10	99.0	−23.0	5.69	14.92	0.657	1.99
	15	94.0	−20.7	3.90	584.79	0.965	1.05
	20	89.2	−19.3	3.84	577.43	0.973	1.04
8% Clo10A	2.5	113.7	−33.3	4.47	0.250	0.036	6.00
	5	104.4	−26.9	4.97	0.958	0.249	3.85
	10	97.0	−20.9	5.98	6.72	0.606	2.20
	15	92.2	−19.7	3.30	469.14	0.951	1.12
	20	87.1	−15.4	3.88	374.46	0.952	1.17

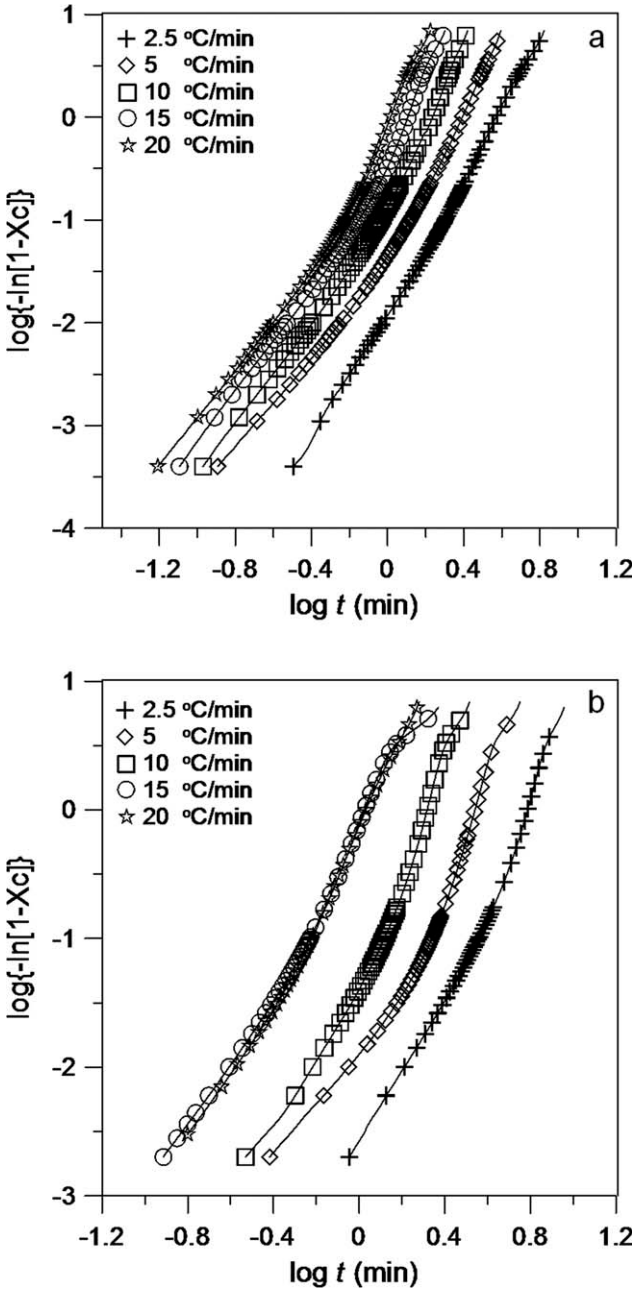

Figure 5 Avrami plots for nonisothermal crystallization of PLLA/PMMA/PEO (80/10/10): (a) +3% OVMT and (b) +3% Clo10A at various cooling rates.

determined by Avrami equation should be corrected as follows:

$$\log Z_c = \frac{\log Z_t}{\alpha} \tag{4}$$

where Z_c is the crystallization kinetics rate constant.

Figure 5 shows the Avrami plot for PLLA/PMMA/PEO (80/10/10) with 3% organoclays scanned in nonisothermal fashion at different cooling rates. As evidenced from Figure 5, the plots of $\log\{-\ln[1 - X_c]\}$ vs. $\log t$ for OVMT and Clo10A consist of two or three linear regions, which mean that Avrami equation cannot fully describe the nonisothermal crystallization of ternary polymer blend nanocomposites. However, the linear portion of the curves covers wide range of relative crystallinity (0.25–0.8) fractions, thus the modified Avrami equation can satisfy the data analysis to some extent.[29,30] Tables I and II summarize the modified Avrami parameters data for nonisothermal crystallization of ternary polymer blend with OVMT and Clo10A, respectively. There is no certain trend for n values along with increasing clay loading or with increasing cooling rates. The values vary from 3.50 to 6.20 for OVMT and 3.30 to 6.68 for Clo10A. The values of n for nanocomposites with OVMT and Clo10A vary from below 4.0 to above it. Most of the values are above than 4.0, which indicate that the nucleation process is very complicated. Z_t and Z_c show the increased values as cooling rate increases, which is reasonable, because Z_t and Z_c measures the crystallization rate which gets faster with supercooling. Z_t is a raw measure of the kinetics of crystallization (i.e., rate constant), while Z_c attempts to quantify the crystallization rate constant after removing the kinetic effect of the nonisothermal cooling conditions under which the crystallization experiments are performed.[31] Z_t and Z_c values tend to decrease with increasing OVMT loading. The decrease of Z_t and Z_c values indicates that the further addition of OVMT from 1% loading leads to decreased crystallization kinetics until some extent. Meanwhile, Z_t and Z_c values for Clo10A are initially increasing with increase of Clo10A loading and then decreases at 3–5 wt % Clo10A loading. The increasing Z_c with Clo10A loading indicates that further addition of Clo10A from 1 wt % increases the crystallization kinetics. The extent of crystallization kinetics is increased until some extent that the further addition of Clo10A retards the crystallization kinetics of ternary polymer blend. Therefore, at low loading, OVMT and Clo10A have opposite effect on the crystallization kinetics of the ternary polymer blend. The $t_{1/2}$ for polymer nanocomposites is shorter at higher cooling rates, as higher cooling rates mean shorter time for crystallization process. Higher cooling rate also induces faster degree of supercooling, thus the crystallization rate is increased. The variation of $t_{1/2}$ with the organoclay loading also shows the same trend as that of Z_c.

Considering the effect of cooling rate on the nonisothermal crystallization, Ozawa[32] has extended the Avrami theory from isothermal crystallization to the nonisothermal crystallization case. The modified Avrami equation (termed as the Ozawa equation) then was described as follows:

$$\log[-\ln(1 - X_c)] = \log K(T) - m \log \alpha \tag{5}$$

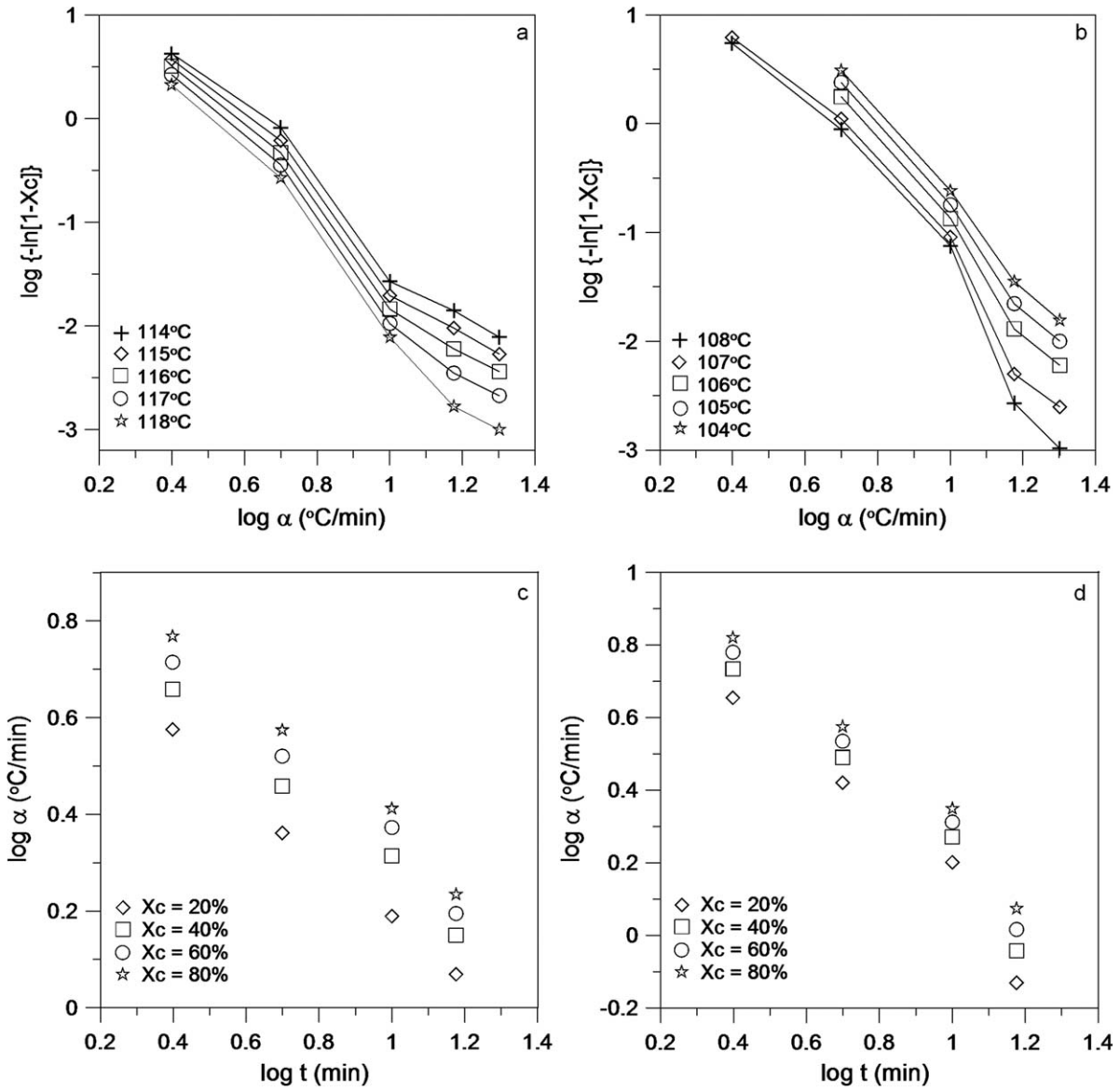

Figure 6 Ozawa plots (upper) and Mo plot (lower) for nonisothermal crystallization of PLLA/PMMA/PEO (80/10/10): (a, c) +3% OVMT and (b, d) +3% Clo10A at various cooling rates.

where $K(T)$ is a cooling function depending on the crystallization rate, and m is the Ozawa exponent depending on the dimension of crystal growth. If Ozawa modification can accurately describe the nonisothermal crystallization kinetics, then the plot of $\log[-\ln(1 - X_c)]$ vs. $\log \alpha$ will yield a straight line. Figure 6, in upper graphs, presents Ozawa plot for ternary polymer blend with 3% OVMT and 3% Clo10A. The plot shows a poor linearity, and the linearity is even worse at higher cooling rate. Under nonisothermal crystallization, the crystallization rate is no longer a constant but a function of both time and cooling rate. If the cooling rates vary in a large range and large amount of crystallization occurs as a result of secondary processes, the Ozawa model would not be adequate in describing nonisothermal crystallization behaviors.[32] Moreover, in Ozawa's theory, the secondary crystallization and the dependence of the fold length on temperature is disregarded. Therefore, the modified Avrami and Ozawa cannot accurately describe the nonisothermal crystallization kinetics of ternary polymer blend with OVMT. Mo and coworkers[33,34] proposed a combined Avrami and Ozawa equation to describe the nonisothermal crystallization kinetics of polymers, as follows:

$$\log Z_t + n \log t = \log K(T) - m \log \alpha \quad (6)$$

$$\log \alpha = \log F(T) - b \log t \quad (7)$$

where the parameters of $F(T)$ and b are equal to $[K(T)/Z_t)]^{1/m}$ and n/m, respectively. The Mo

TABLE III
Parameters of PLLA/PMMA/PEO (80/10/10)+OVMT Nanocomposites Using Nonisothermal Crystallization Analysis with Mo's Method

Clay loading	X_c (%)	Log $F(T)$	b
1% OVMT	20	0.84	0.64
	40	0.91	0.62
	60	0.96	0.62
	80	1.01	0.63
3% OVMT	20	0.82	0.64
	40	0.91	0.63
	60	0.97	0.64
	80	1.04	0.66
5% OVMT	20	0.93	0.70
	40	1.03	0.72
	60	1.09	0.74
	80	1.14	0.74
8% OVMT	20	0.88	0.62
	40	1.00	0.66
	60	1.07	0.69
	80	1.14	0.71
1% Clo10A	20	1.17	1.03
	40	1.21	0.98
	60	1.23	0.95
	80	1.24	0.92
3% Clo10A	20	1.07	0.95
	40	1.14	0.95
	60	1.18	0.94
	80	1.21	0.92
5% Clo10A	20	0.91	0.80
	40	1.05	0.84
	60	1.11	0.86
	80	1.16	0.85
8% Clo10A	20	1.05	0.89
	40	1.15	0.90
	60	1.20	0.89
	80	1.23	0.87

equation correlates the cooling rate and the crystallization time under nonisothermal crystallization condition and could be defined by a certain degree of crystallinity. The physical meaning of $F(T)$ is the value of cooling rate, chosen at a unit crystallization time when the system arrives at certain degree of crystallinity.[35] Figure 6, lower graphs, presents the plot of Mo model for polymer nanocomposites with 3% OVMT and 3% Clo10A. From the plot, a good linearity is obtained, indicating that the Mo model could describe nonisothermal crystallization process for this system accurately. From the linearity, the crystallization kinetics parameters $F(T)$ and b can be obtained. The results are presented in Table III.

From the data, it is shown that the values of $F(T)$ increase with increasing degree of crystallinity, which indicates higher cooling rate is needed to obtain higher degree of crystallinity. The values of b are almost constant in each organoclay loading. The value of $F(T)$ is increased with increasing OVMT loading at certain degree of crystallinity. The higher $F(T)$ means that the higher cooling rate or higher crystallization rate is needed. If the higher crystallization rate is needed to arrive at certain degree of crystallinity, it means that greater effort must be made to reach the same degree of crystallinity. In other words, the barrier to be overcome is higher. Therefore, higher OVMT loading from 1 wt % directly leads to the higher barrier or higher retardation effect. Meanwhile, the trend for Clo10A loading is the opposite of OVMT. Increasing the Clo10A loading to above 1 wt % will increase the crystallization process to some extent, which is indicated by decreasing $F(T)$ value. These trends are in a good agreement with kinetics analysis from the Avrami method. However, the values of $F(T)$ in OVMT samples at the same loading are significantly lower than that of Clo10A. This indicates that OVMT is more superior to Clo10A in enhancing crystallization process of ternary polymer blend, despite of the different trend of organoclay loading on crystallization process.

It should be postnoted that results opposite to the above may also be present. In a recent study, it was found that the addition of nanoclays does not enhance the crystallization behavior of PLA.[36] The ternary blend matrix in this study contains PMMA and PEO, which retard the crystallization of PLLA. On loading the clay into the ternary blend, the retarded crystallization may be reversed. It should be pointed out that PLA's have various molecular weights, and their crystallization rates differ significantly. All various studies in the literature point a conclusion that experimental evidence of crystallization should be verified for each individual matrix/clay system.

Enzymatic and thermal degradation of ternary polymer blend nanocomposites

Enzymatic degradation is an important test to assess the biodegradable properties of polymers. PLA is known to be degraded by Proteinase K enzymes,[12,37–40] as it catalyzes the hydrolysis L-lactide unit sequences in PLA.[41] As both OVMT and CloA are well dispersed in the ternary polymer blend matrix, it is interesting to investigate the degradation of the polymer nanocomposites. Figure 7 shows the SEM micrographs for degraded samples of neat polymer blend and its nanocomposites. After enzymatic degradation course for 30 h, the extent of surface roughness is different between each sample. From the SEM figure, many cracks and holes are present in the samples owing to enzyme degradation, where the roughness of nanocomposites' surface is somehow lower than that of neat polymer blend. The roughness of samples with OVMT is much different than that of Clo10A. Apparently, the samples of Clo10A show higher extent of degradation.

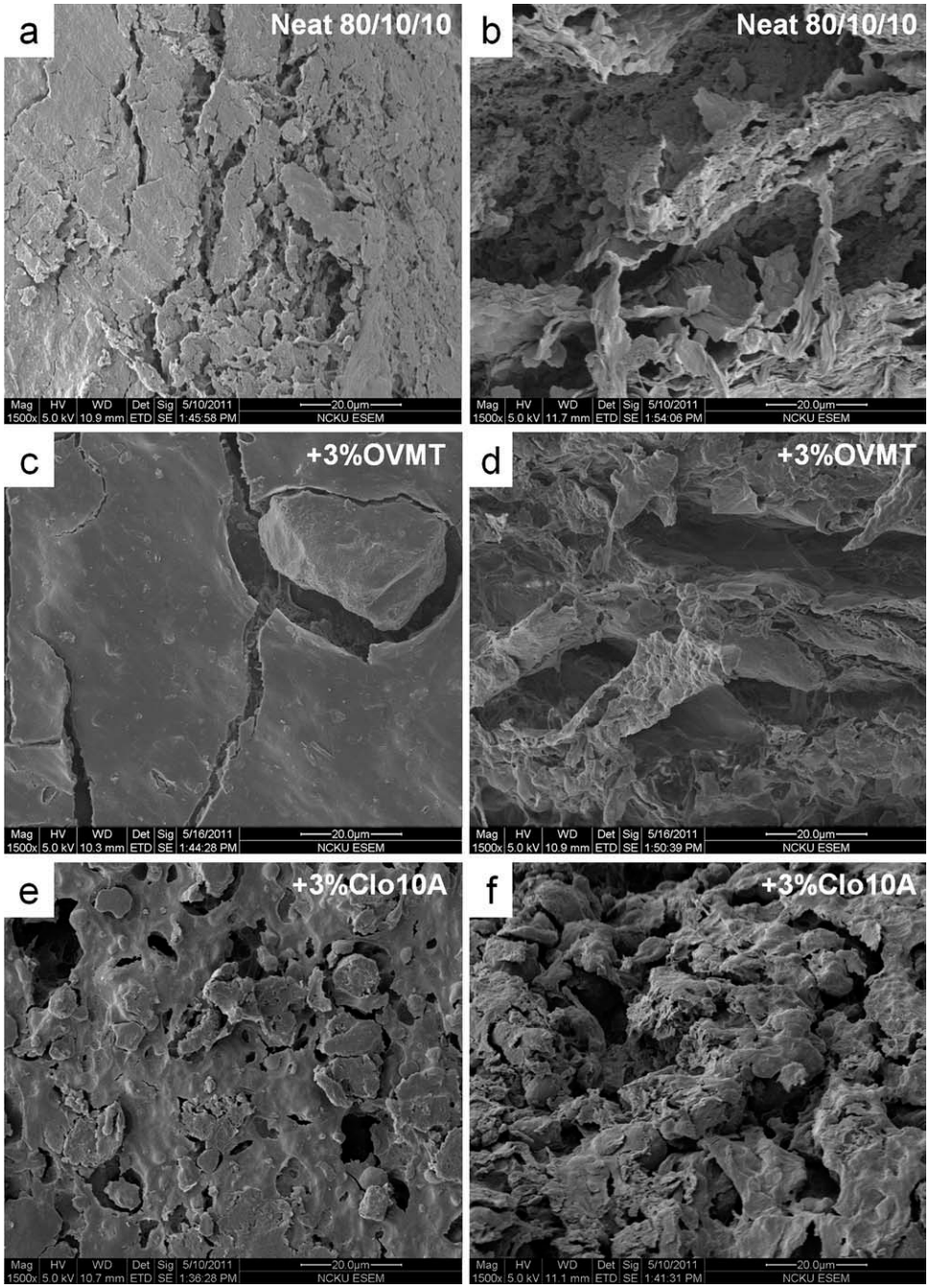

Figure 7 SEM micrographs of top surface (left side) and side surface (right side) after 30 h degradation of PLLA/PMMA/PEO (80/10/10) blend matrix: (a, b) neat blend, (b, c) blend +3% OVMT, and (e, f) blend +3% Clo10A.

To assess the degradation extent, the weight loss curves for the neat polymer blend (0% clay) and its nanocomposites (1–8 wt % clay of either OVMT or Clo10A) in enzymatic solutions are presented in Figure 8. As shown in the figure, the enzymatic weight loss of all polymer nanocomposites is lower than that of neat polymer blend, and the weight loss decreases as organoclays loading increases. The nanocomposite sample with 8% clay may show some scattering out of the general trend, but within 8 wt % clay loading in the matrix, the trend of effect of nanoparticles is quite consistent. This result indicates that the incorporation of clay retards the enzymatic degradation. Enzymatic degradation is surface erosion which hardly affects the bulk properties. Several researchers reported surface erosion process as enzymatic degradation takes place in PLLA single crystals by Proteinase K,[42] PCL-PLLA block or random copolymers during degradation by pseudomonas lipase,[43,44] and PLLA-corn starch biocomposites by Proteinase K.[45] Generally, the enzymatic degradation is faster in the presence of the amorphous

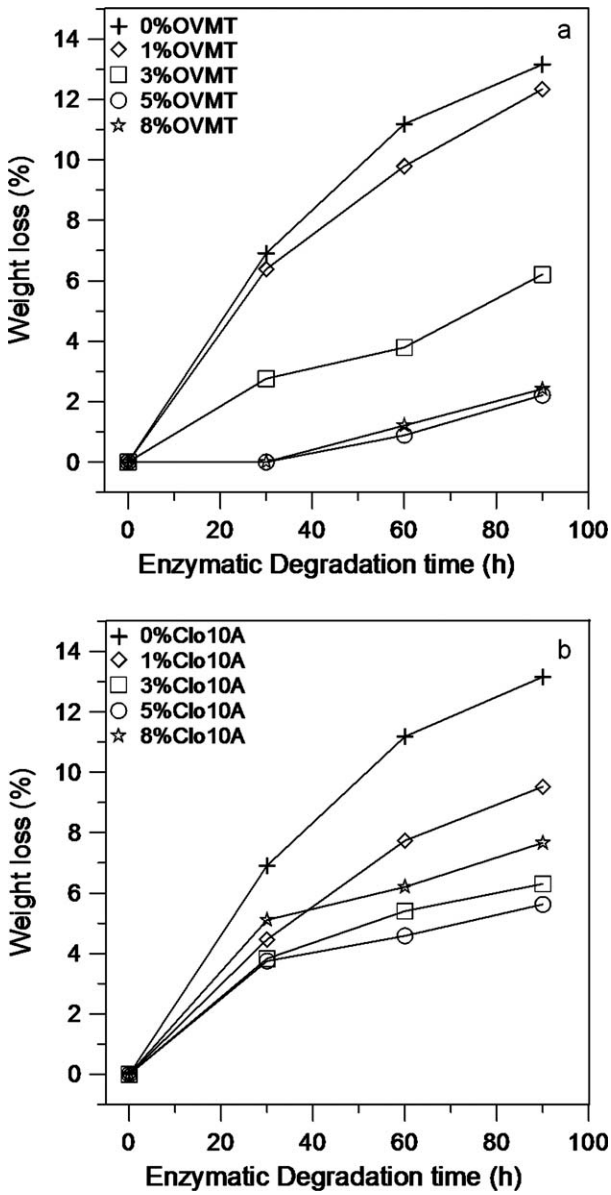

Figure 8 Comparison of weight losses by enzymatic degradation course for polymer nanocomposites with: (a) OVMT and (b) Clo10A.

regions, as it is easier to attack than the crystalline one. Because both OVMT and Clo10A have the same trend on the clay loading during enzymatic degradation process, which is the opposite as the trend on crystallization kinetics, it seems that the crystallinity is not the main cause of their lower degradation rate. Note that the OVMT and Clo10A have the opposite trend on crystallization, while on enzymatic degradation their trend is same. Fukuda et al.[46,47] reported that the enzymatic degradation activity was affected by surface treatment. Several researchers also suggested that surface modification and interfacial adhesion of filler affects the enzymatic degradation process.[48] The difference of degradation extent between OVMT and Clo10A may be due to the modifier used. The polymer nanocomposites with OVMT seem to have better interaction (organophilicity) with ternary polymer blend matrix than that of Clo10A. Therefore, the interaction between clay and polymer blend matrix is stronger, thus hindering the enzymatic attack on PLLA chain more than Clo10A. The bouncing effect of degradation extent for Clo10A can be attributed to the tendency of agglomeration of organoclay at high loading, thus reducing their interaction with polymer matrix. Therefore, at high Clo10A loading, the enzymatic degradation is increased.

Some contradictory confusion may appear in the data for 8 wt % clay (high clay loading) in the ternary blend matrix. In a recent study, it has been pointed out that the clay in aliphatic polyesters may not exhibit such an effect on hydrolysis.[49] The general trend shows that clay in blend matrix retards enzymatic degradation for clay loading below 8 wt %. It seems that the effect of nanoclays on hydrolysis may be dependent on component of sample matrix. In this case, it should be emphasized that the matrix contains a water-soluble component of PEO, which may expedite the rate as clay loading is above a limit (in this case 8 wt %).

In addition to enzymatic degradation, thermal stability of the nanocomposites in comparison with the ternary blend matrix was also evaluated. Figure 9 presents the TGA and DTG (differential of TGA) curves for polymer nanocomposites. For all polymer nanocomposites, the thermal stability is enhanced by the incorporation of organoclays. The temperature for 5% weight loss for neat (without organoclay) ternary polymer blend ($T_{5\%}$) is around 276.6°C. On incorporation of organoclays, the starting degradation temperature (T_{on}) is also shifted to higher temperature. The characteristic temperatures for thermal degradation are summarized in Table IV. For polymer nanocomposites with OVMT, the increasing clay loading leads to the shifts of characteristic temperatures to higher scale. But, after 5% OVMT loading, all characteristic temperatures are drop to lower value, as evident from Figure 9(a). From Figure 9(c), it is shown that no significant change in temperature corresponding to the maximum rate of weight loss (T_p) at 1% OVMT loading. During degradation course, the sample with 5% OVMT loading shows the best thermal stability.

Regarding the characteristic temperatures presented in Table IV, incorporation of OVMT shift $T_{5\%}$ up to 29.4°C, which is obtained by 5% OVMT loading. The residue at 800°C shows monotonic increase along with organoclay content in the samples. This monotonic trend is also observed in samples containing Clo10A. Figure 9(b,d) present TGA and DTG curves for polymer nanocomposites with Clo10A. Upon addition 1% Clo10A, the thermal stability of

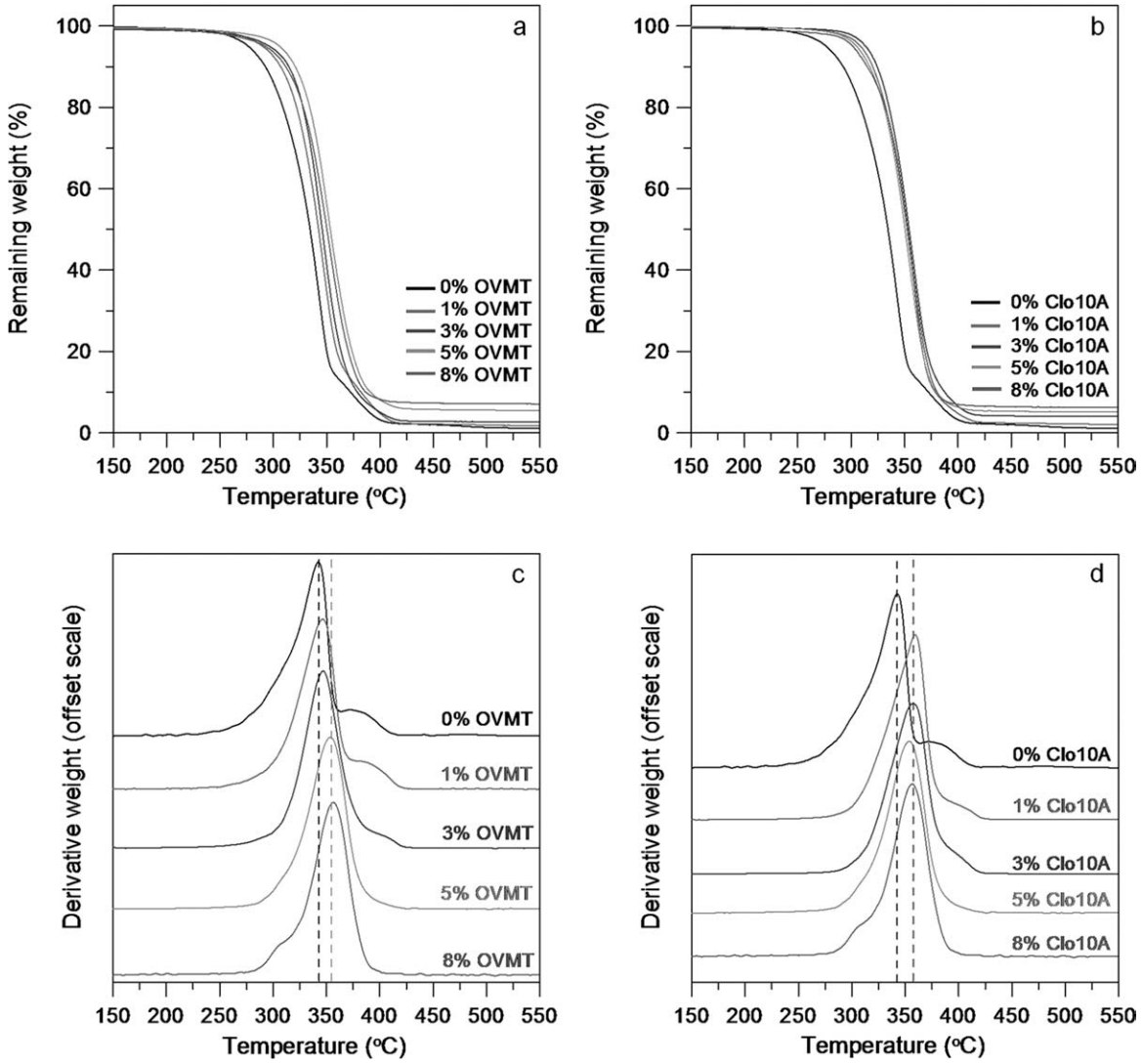

Figure 9 TGA (upper) and DTG (lower) curves for PLLA/PMMA/PEO (80/10/10) and its nanocomposites with OVMT (a, c) and Clo10A (b, d).

the polymer nanocomposites is greatly enhanced. However, the thermal stability is lowered when Clo10A loading reaches 5 wt % or higher. From Table IV, the maximum extent of thermal stability is obtained by 3% Clo10A loading which results in the increase of 36.9°C in $T_{5\%}$. Therefore, Clo10A is superior to OVMT in enhancing the thermal stability of ternary polymer blend. In Figure 9(c,d), for DTG curves, it is clearly shown that the neat ternary polymer blend degraded in two stages, because there are two peaks in the curves. Under inert gas, PLLA is generally thermally degraded in one step as Wen et al.[48] have observed two-step thermal degradation of neat PLA under air environment. As the ternary polymer blend system is mainly composed of PLLA, probably the presence of PMMA induces two steps degradation process for ternary polymer blend. The degradation of PMMA takes place around 370°C. This seems reasonable, because the second stage takes place at around 10% remaining weight of polymer nanocomposites. On further addition of organoclays, the second peak in DTG curves is suppressed

TABLE IV
Characteristic Thermal Degradation Temperatures of Ternary PLLA/PMMA/PEO Blends Filled with Organoclays

	$T_{5\%}$ (°C)	$T_{10\%}$ (°C)	T_p (°C)	Residue at 800°C (wt %)
Neat	276.6	292.5	343.3	1.71
1% OVMT	290.0	306.9	346.5	2.06
3% OVMT	296.3	314.5	347.0	2.52
5% OVMT	306.0	320.5	353.6	4.86
8% OVMT	292.5	311.7	356.5	6.42
1% Clo10A	308.8	320.1	359.4	2.03
3% Clo10A	313.5	324.3	357.4	3.70
5% Clo10A	305.1	317.3	353.6	4.77
8% Clo10A	301.4	314.9	356.5	5.69

and finally disappears at 5% organoclays loading. This may due to the barrier effect induced by the organoclays, which prevents the diffusion of volatile decomposition products out of the polymer during thermal degradation.

Two recent reviews by Bikiaris and coworkers[50,51] in the area of effects of clays in thermal stability of polymer matrices have indicated that that the used amount of clays has a substantial effect of PLA thermal stability. At a low fraction of clay particles to the polymer matrices, the clay layers are well dispersed, and the barrier effect is predominant. By contrast, with increasing clay loading, the effect may be reversed and the thermal stability of the nanocomposites starts to decrease at clay loadings exceeding a limit. Such views are in agreement with the finding in the nanocomposite systems in this study.

CONCLUSION

In continuing a previous study dealing with VMT-clay based nanocomposites,[21] this study further extended to another common clay (Cloisite) to compare the properties, kinetics, and bio- and thermal degradability of two different clays based on the same ternary blend matrix. Two different organoclays were incorporated to ternary polymer blend as matrix composed of PLLA, PMMA, and PEO. The addition of PMMA into PLLA/PEO reduces chain mobility and retards the crystallization of PLLA. The retardation effect of PMMA is expelled by the addition of organoclays. Both OVMT and Clo10A enhances the nonisothermal crystallization of ternary polymer blend dramatically, because the ternary polymer blend is hardly crystallize from the melt even with cooling rate as low as 2.5°C/min. The kinetics of nonisothermal process was well described by Mo method. Each of the organoclays induces different trend on nonisothermal crystallization with respect to its loading. Further addition of OVMT from 1 wt % loading retards the crystallization process, while Clo10A enhances the crystallization process to some extent before retarding it. However, the nucleation and crystallization extent induced by OVMT is superior to that of Clo10A. The evolution of activation energy also shows the same trend as crystallization process. Higher content of OVMT directly increases the activation energy, while Clo10A reduces it to some extent.

The addition of organoclays generally decreases the enzymatic degradation of ternary polymer blend. By comparison, enzymatic degradation tests on the Clo10A composite show that it has better degradation property than that of OVMT. This may be due to different organic modifier used to modify the surfaces of the clays. TGA thermal degradation analyses show that both OVMT and Clo10A exhibit improvement in thermal stability. Generally, composite samples with Clo10A have better thermal stability than that of OVMT. Maximum extent of enhancing thermal stability is achieved by sample with 3% Clo10A loading and 5% OVMT loading, respectively. Therefore, by adjusting the organoclay loading and ternary polymer matrix, the crystallization process as well as thermal property, and degradability of ternary polymer blend nanocomposites can be optimized or controlled for objectives.

A. Auliawan, an Indonesia national, is funded by Taiwan Government Scholarship for his M.S. degree study at National Cheng Kung University (NCKU), Tainan, Taiwan.

References

1. Bordes, P.; Pollet, E.; Averous, L. Prog Polym Sci 2009, 34, 125.
2. Zhang, J.; Xu, J.; Wang, H.; Jin, W.; Li, J. Mat Sci Eng C 2009, 29, 889.
3. Sangwan, P.; Way, C.; Wu, D. Y. Macromol Biosci 2009, 9, 677.
4. Sawyer, D. J. Macromol Symp 2001, 201, 271.
5. Drumright, R. E.; Gruber, P. R.; Henton D. E. Adv Mater 2000, 12, 1841.
6. Dorgan, J. R.; Lehermeier, H. J.; Palade, L. I.; Cicero, J. Macromol Symp 2001, 175, 55.
7. Ikada, Y.; Tsuji, H. Macromol Rapid Commun 2000, 21, 117.
8. Garlotta, D. J Polym Environ 2002, 9, 63.
9. Fukushima, K.; Tabuani, D.; Camino, G. Mat Sci Eng C 2009, 29, 1433.
10. Ronneberger, B.; Kao, W. J.; Anderson, J. M.; Kissel, T. J Biomed Mater Res 1996, 30, 31.
11. Nishino, S.; Kitamura, Y.; Kishida, A.; Yoshizawa, H. Macromol Biosci 2005, 5, 1066.
12. Agari, Y.; Sakai, K.; Kano, Y.; Nomura, R. J Polym Sci Part B: Polym Phys 2007, 45, 2972.
13. Moussaif, N.; Groeninckx, G. Polymer 2003, 44, 7899.
14. Tjong, S. C. Mater Sci Eng R 2006, 53, 73.
15. Xu, J.; Li, R. K. Y.; Xu, Y.; Li, L.; Meng, Y. Z. Eur Polym J 2005, 41, 881.
16. Tjong, S. C.; Meng, Y. Z.; Xu, Y. J Polym Sci Part B: Polym Phys 2002, 40, 2860.
17. Zhang, K.; Xu, J.; Wang, K. Y.; Cheng, L.; Wang, J.; Liu, B. Polym Degrad Stab 2009, 94, 2121.
18. Zhang, Y.; Han, W.; Wu, C. F. J Macromol Biosci B 2009, 48, 967.
19. Mittal, V. J Compos Mater 2008, 42, 2829.
20. Shieh, Y. T.; Liu, G. L. J Polym Sci Part B: Polym Phys 2007, 45, 466.
21. Auliawan, A; Woo, E. M. Polym Compos 2011, 32, 1916.
22. Xue, M. L.; Sheng, J.; Yu, Y. L.; Chuah, H. H. Eur Polym J 2004, 40, 811.
23. Papageorgiou, G. Z.; Achilias, D. S.; Bikiaris, D. N. Macromol Chem Phys 2007, 208, 1250.
24. Qin, J.; Guo, S.; Li, Z. J Appl Polym Sci 2008, 109, 1515.
25. Gopakumar, T. G.; Lee, J. A.; Kontopoulou, M.; Parent, J. S. Polymer 2002, 43, 5483.
26. Xu, W.; Ge, M.; He, P. J Appl Polym Sci 2001, 82, 2281.
27. Xu, W.; Ge, M.; He, P. J Polym Sci Part B: Polym Phys 2002, 40, 408.
28. Supaphol, P. J Appl Polym Sci 2000, 78, 338.
29. Joshi, M.; Butola, B. S. Polymer 2004, 45, 4953.

30. Mitchell, C. A.; Krishnamoorti, R. Polymer 2005, 46, 8796.
31. Jiang, C.; Wang, D.; Zhang, M.; Li, P.; Zhao, S. Eur Polym J 2010, 46, 2206.
32. Ozawa, T. Polymer 1971, 12, 150.
33. Liu, T.; Mo, Z.; Wang, S.; Zhang, H. Polym Eng Sci 1997, 37, 568.
34. Liu, M.; Zhao, Q.; Wang, Y.; Zhang, C.; Mo, Z.; Cao, S. Polymer 2003, 44, 2537.
35. Liu, X.; Wu, Q. Eur Polym J 2002, 38, 1383.
36. Papageorgiou, G. Z.; Achilias, D. S.; Nanaki, S.; Beslikas, T.; Bikiaris, D. Thermochim Acta 2010, 511, 129.
37. Zhao, Y. Q.; Cheung, H. Y.; Lau, K. T.; Xu, C. L.; Zhao, D. D.; Li, H. L. Polym Degrad Stab 2010, 95, 1978.
38. Reeve, M. S.; McCarthy, S. P.; Downey, M. J.; Gross, R. A. Macromolecules 1994, 27, 825.
39. Tsuji, H.; Miyauchi, S. Polym Degrad Stab 2001, 71, 415.
40. Tsuji, H.; Kidokoro, Y.; Mochizuki, M. Macromol Mater Eng 2006, 291, 1245.
41. MacDonald, R. T.; McCarthy, S. P.; Gross, R. A. Macromolecules 1996, 29, 7356.
42. Iwata, T.; Doi, Y. Macromolecules 1998, 31, 2461.
43. Li, S. M.; Liu, L. J.; Garreau, H.; Vert, M. Biomacromolecules 2003, 4, 372.
44. Zhao, Z. X.; Yang, L.; Hu, Y. F.; He, Y.; Wei, J.; Li, S. M. Polym Degrad Stab 2007, 92, 1769.
45. Ohkita, T.; Lee, S. H. J Appl Polym Sci 2006, 100, 3009.
46. Fukuda, N.; Tsuji, H.; Ohnishi, Y. Polym Degrad Stab 2002, 78, 119.
47. Fukuda, N.; Tsuji, H. J Appl Polym Sci 2005, 96, 190.
48. Wen, X.; Zhang, K.; Wang, Y.; Han, L.; Han, C.; Zhang, H.; Chen, S.; Dong, L. Polym Int 2011, 60, 202.
49. Vassiliou, A. A.; Bikiaris, D.; El Mabrouk, K.; Kontopoulou, M. J Appl Polym Sci 2011, 119, 2010.
50. Chrissafis, K.; Bikiaris, D. Thermochim Acta 2011, 53, 1.
51. Bikiaris, D. Thermochim Acta 2011, 53, 25.